J. Hydrol. Hydromech., 66, 2018, 4, 360–368
DOI: 10.2478/johh-2018-0024

Extent and persistence of soil water repellency induced by pines in different geographic regions

Massimo Iovino[1*], Pavla Pekárová[2], Paul D. Hallett[3], Ján Pekár[4], Ľubomír Lichner[2], Jorge Mataix-Solera[5], Vincenzo Alagna[1], Richard Walsh[3], Annette Raffan[3], Karsten Schacht[6], Marek Rodný[2]

[1] Dipartimento di Scienze Agrarie, Alimentari e Forestali, Università degli Studi di Palermo, Viale delle Scienze, Ed. 4 Ingr. E, 90128 Palermo, Italy.
[2] Slovak Academy of Sciences, Institute of Hydrology, Dúbravská cesta 9, 84104 Bratislava, Slovakia.
[3] University of Aberdeen, Institute of Biological & Environmental Sciences, Aberdeen AB24 3UU, United Kingdom.
[4] Comenius University, Faculty of Mathematics, Physics and Informatics, Mlynská dolina 1, 842 48 Bratislava, Slovakia.
[5] Departamento de Agroquímica y Medio Ambiente, Universidad Miguel Hernández, Edificio Alcudia, Avda de la Universidad, 03202 Elche Alicante, Spain.
[6] Department of Soil Science and Soil Ecology, Institute of Geography, Ruhr-Universitat Bochum, Universitatsstrasse 150, 44801 Bochum, Germany.
[*] Corresponding author. Tel.: +39 091 23897070. Fax: +39 091 484035. E-mail: massimo.iovino@unipa.it

Abstract: The extent (determined by the repellency indices RI and RI_c) and persistence (determined by the water drop penetration time, WDPT) of soil water repellency (SWR) induced by pines were assessed in vastly different geographic regions. The actual SWR characteristics were estimated *in situ* in clay loam soil at Ciavolo, Italy (CiF), sandy soil at Culbin, United Kingdom (CuF), silty clay soil at Javea, Spain (JaF), and sandy soil at Sekule, Slovakia (SeF). For Culbin soil, the potential SWR characteristics were also determined after oven-drying at 60°C (CuD). For two of the three pine species considered, strong (*Pinus pinaster* at CiF) and severe (*Pinus sylvestris* at CuD and SeF) SWR conditions were observed. *Pinus halepensis* trees induced slight SWR at JaF site. RI and RI_c increased in the order: JaF < CuF < CiF < CuD < SeF, reflecting nearly the same order of WDPT increase. A lognormal distribution fitted well to histograms of RI_c data from CuF and JaF, whereas CiF, CuD and SeF had multimodal distributions. RI correlated closely with WDPT, which was used to develop a classification of RI that showed a robust statistical agreement with WDPT classification according to three different versions of Kappa coefficient.

Keywords: Pine; Soil; Water repellency; Water drop penetration time; Repellency index.

INTRODUCTION

Pines are widely planted for sand dune stabilization (CAB International, 2002; Islam et al., 2011; Janusauskaite et al., 2013), but there is a common misconception discounted by scientific evidence that pure coniferous forests cause serious and irreversible soil deterioration. Where deterioration on soils by coniferous forests has been observed it has largely been caused by man's mismanagement and exploitation (Will and Raliard, 1976).

Pine species, having considerable quantities of resins, waxes and aromatic oils in their needles and bark, can induce soil water repellency (SWR) (Doerr et al., 2000; Garcia et al., 2005), resulting in a change to soil hydrophysical properties. Pine root excreted mucilages containing aliphatic compounds may also contribute to SWR (Rumpel et al., 1998). SWR can develop in soils of different textural composition and structural properties, and has been found all over the world (Beatty and Smith, 2010, 2013; Fér et al., 2016; Ward et al., 2015). It can impede infiltration of water, promote surface runoff and erosion, and give rise to preferential flow of water and accelerated transport of chemicals into the groundwater (Doerr et al., 2000; Lichner et al., 2013; Orfánus et al., 2008). Moreover, by modifying water availability, SWR indirectly affects seed germination, seedling establishment and plant growth (Siteur et al., 2016). The impact of pines on soil properties is the result of interactions between the trees and the different components of the ecosystem (Bens et al., 2006, 2007). SWR in forest soils depends on tree species, age of the forest, season of the year, soil water content, organic matter content and type, clay content, wetting and drying history of the soil, frequency of fires, temperature, and relative ambient air humidity (Buczko et al., 2002, 2005, 2006; Diehl, 2013; Doerr et al., 2000; Flores-Mangual et al., 2013). The impacts can be spatially variable, as observed by Gerke et al. (2001) for potential water repellency in a lignitic mine soil afforested with *Pinus nigra.*

SWR is characterized by its persistence (estimated by the water drop penetration time (WDPT) test), severity (measured by the molarity of an ethanol droplet (MED) test, as well as from the water-solid contact angle and capillary rise measurements), and extent (determined by the repellency index RI) (Haas et al., 2018; Krueger et al, 2018; Lichner et al., 2018). The SWR characteristics can be both spatially and temporally variable. From small-scale (centimetre and decimetre) measurements using micro- (disk radius of 1.4 mm) and mini-disk infiltrometers (disk radius of 22.5 mm) at sampling interval of 5 cm and 10 cm, respectively, found water sorptivity S_w could vary by an order of magnitude between neighbouring measuring points (Hallett et al., 2004; Lichner et al., 2012). Such as large amount of spatial variability hinders the measurements of RI as paired measurements of S_w and ethanol S_e sorptivity are needed (Keck et al., 2016; Lichner et al., 2007, 2010). This can be overcome using a combined repellency index RI_c (Alagna et al., 2017), calculated according to Pekárová et al.'s (2015) method by taking into account all the combinations of the measured S_w and S_e pairs. Orfánus et al. (2008) found similar small-scale variation of WDPT.

An assessment of different methods to measure SWR has not yet been reported. For pine soils this is important due to widespread occurrence of SWR, which Rodriguez-Alleres and Benito (2011) found to vary considerably both spatially and temporally on the surface of sandy loam soils of NW Spain under *Pinus pinaster* plantations. The relationship between different measurements and their spatial variability is also important, as RI and MED measure the extent, whereas WDPT reports the persistence of water repellency. Doerr (1998) determined the comparability of MED and WDPT results using air-dried soils with a broad particle size and hydrophobicity range. A close relationship between the two tests was found for highly hydrophobic soils, but not for moderately hydrophobic soils. Whether different SWR measurements are comparable spatially is not known.

The objective of this study was to assess the extent and persistence of soil water repellency induced by pines in vastly different geographic regions. The actual water repellency characteristics were estimated in situ in Ciavolo, Italy, Culbin, United Kingdom, Javea, Spain, and Sekule, Slovakia. Due to its high wettability in the field, the potential water repellency characteristics were also determined after oven-drying at 60°C for Culbin soil. The second objective of this study was to propose a classification of the repellency index RI and determine the comparability of RI and WDPT results.

MATERIAL AND METHODS

Study sites

The first experimental site is located in Ciavolo on the island of Sicily, Italy (37°45'40.6" N, 12°34'09.0" E), under a 30 years old *Pinus pinaster* tree canopy that fully covers the soil surface (site CiF). This area is representative of the reforestations widely applied in the past decades to tackle land degradation. According to the Köppen-Geiger climate classification, the region is classified as Mediterranean, hot summer (Csa) (Kottek et al., 2006). Warm and dry periods in summer alternate with heavy rainfalls mostly occurring in autumn and winter. The average annual rainfall is 632 mm. The elevation at the experimental site is 105 m a.s.l. and the surface slope is shallow (4.4%). The soil is a Rhodoxeralf (Soil Survey Staff, 2014) with a depth of 0.40–0.60 m and the parent material is calcareous sandstone. According to USDA classification, the soil texture is clay loam (Gee and Bauder, 1986). The mean volumetric soil water content at the time of sampling was 0.160 $cm^3\,cm^{-3}$.

The second experimental site was Culbin forest located in the north of Scotland on the southern shore of the Moray Firth (57.63° N, 3.72° W). According to the Köppen-Geiger climate classification, the region is classified as temperate oceanic climate (Cfb) (Kottek et al., 2006) with average annual rainfall of 665 mm. Elevation at the experimental site is 5 to 20 m a.s.l. with slopes ranging from 0 to 18%. Culbin forest was once an area of unstable sand dunes produced by windblown sand from raised beaches west of the site (Ovington, 1950). The forest was planted in 1888 to physically stabilise dune sands. The primary species planted in Culbin forest are Scots pine (*Pinus sylvestris*) and Corsican pine (*Pinus nigra*). The soil is an Ustoxic Quartzipsamments (Soil Survey Staff, 2014) comprised of an organic surface layer overlaying windblown sand. According to USDA classification, the soil texture is sandy (Gee and Bauder, 1986). Soils were sampled at the interface between the organic layer and mineral soil, at a depth of 50 mm from the surface. An assessment of the actual water repellency characteristics was conducted *in situ* (CuF) whereas potential water repellency characteristics were determined in laboratory after oven-drying at 60°C (CuD).

The third experimental site is located at Javea close to Alicante, Spain (38°48'15.0" N, 0°09'18.8" E, elevation 213 m a.s.l.), in a 40 years old afforested plantation of *Pinus halepensis* (Site JaF). The region is classified as Mediterranean, hot summer (Csa) (Kottek et al., 2006). The average annual rainfall is 583 mm, which is mainly winter-dominant. In the past, the site was cultivated as shown by the presence of abandoned agricultural terraces. The soil is a Lithic Rhodoxeralf (Soil Survey Staff, 2014) developed over a karstified limestone with variable depth, generally lower than 0.5 m. According to USDA classification, the soil is silty clay (Gee and Bauder, 1986). The mean volumetric soil water content at the time of sampling was 0.082 $cm^3\,cm^{-3}$.

The fourth experimental site is located at Sekule (48°37'10'' N, 17°00'10'' E) in the Borská nížina lowland (southwest Slovakia), under a 30 years old Scots pine (*Pinus sylvestris*) tree canopy that fully covers the soil surface (site SeF). The region is classified as warm temperate, full humid, cool summer (Cfc) (Kottek et al., 2006). Mean annual precipitation is 550 mm, which is mainly summer-dominant. Elevation is 158 m a.s.l. and surface slope is negligible. The soil is formed by aeolian sand, and it is classified as Aridic Ustipsamments (Soil Survey Staff, 2014). According to USDA classification, soil texture is sandy (Gee and Bauder, 1986). The mean volumetric soil water content at the time of sampling was lower than 0.035 cm^3cm^{-3}. Soil physical and chemical properties of all four sites are presented in Table 1.

Field methods

Field measurements of infiltration were performed with the minidisk infiltrometer (Decagon, 2012) under a negative tension $h_0 = -2$ cm. The soil sorptivity S (L $T^{-0.5}$) was estimated from the cumulative infiltration, I (L), during early-time infiltration process (Philip, 1957):

$$S(-2\text{ cm}) = I / t^{1/2} \tag{1}$$

Equation (1) was used to calculate both the water sorptivity, S_w, and ethanol sorptivity, S_e, i.e., the soil sorptivity when, respectively, water or ethanol is used as infiltrating fluid.

Two methods were used to estimate the repellency index, RI. In the first method of estimating the repellency index, S_e and S_w were measured in pairwise arrangements (Keck et al., 2016; Lichner et al., 2007, 2010) and only one value of the standard

Table 1. Physical and chemical properties of soil samples from the experimental sites: clay loam soil under *Pinus pinaster* trees at Ciavolo, Italy (CiF), sandy soil under *Pinus sylvestris* trees at Culbin, UK (CuF), silty clay soil under *Pinus halepensis* trees at Javea, Spain (JaF), and sandy soil under *Pinus sylvestris* trees at Sekule, Slovakia (SeF) (NA – not available).

Site	Sand (%)	Silt (%)	Clay (%)	$CaCO_3$ (%)	C_{org} (%)	pH (H_2O)	pH ($CaCl_2$)
Ciavolo	23.6	43.0	33.4	2.05	2.49	7.39	6.76
Culbin	97.1	0.7	1.0	0.04	1.23	NA	4.81
Javea	15.7	43.3	40.8	4.11	4.95	7.55	6.78
Sekule	95.1	2.3	2.6	<0.05	0.83	5.65	4.39

repellency index RI was calculated from one pair of S_e and S_w measurements as follows (Hallett et al., 2001):

$$RI = 1.95\, S_e / S_w \quad (2)$$

In the second method of estimating the repellency index, the combination of all the ethanol and water sorptivities was used to calculate a combined repellency index, RI_c, i.e., $m \times n$ values of RI_c were calculated from m values of S_w and n values of S_e (Pekárová et al., 2015).

The persistence of SWR was assessed using the WDPT by placing a drop of distilled water from a standard medicine dropper or pipette on the soil surface and recording the time to complete penetration. A standard droplet release height of approximately 10 mm above the soil surface was used to minimise the cratering effect on the soil surface. The following classes of the persistence of SWR were distinguished: wettable or non-water-repellent soil (WDPT < 5 s), slightly (WDPT = 5–60 s), strongly (WDPT = 60–600 s), severely (WDPT = 600–3600 s), and extremely (WDPT > 3600 s) water repellent soil (Dekker et al., 2000).

To find the relationship between RI/RI_c and WDPT, the number of plots was increased using the results published in Lichner et al. (2012, 2017). The same field methods as outlined above were used in both studies to obtain WDPT and sorptivity data. Data from Lichner et al. (2012) were collected at Sekule in a bare soil with sandy texture. Two depths were sampled: i) surface soil covered with biological soil crust (SeC), and ii) 50 cm depth soil to exclude the impact of vegetation or organic matter (SeS). At each depth, 10 replicated measurements for WDPT and 9 for S_w and S_e were conducted. Five sites were considered in the second study (Lichner et al., 2017) including a loamy sand soil under avocado trees (HaA) at Ha Ma´apil, Israel, a loamy sand soil (NeP1) and a silty clay soil (NeP2) under date palms at Neve Etan, Israel, and a uncultivated bare sandy soil (ShB1, ShB2) at Shafdan, Israel. From 9 to 15 replicated measurements for WDPT and from 7 to 8 for S_w and S_e were conducted depending on the site. An overall set of WDPT, RI, and RI_c data collected from 12 plots was thus considered to find the relationship between RI/RI_c and WDPT.

Statistical methods

To determine the comparability of RI_c results, estimated according to the Pekárová et al. (2015) method, and WDPT results, a wide set of statistical methods were used (e.g. regression analysis, theory of distribution functions, their transformation and characteristics – like means and quantiles). The statistical software STATGRAPHICS (Statgraphics, 2014) was used for computations.

The values of the paired samples were tested by Cohen's unweighted Kappa coefficient, as well as weighted Kappa coefficients (Friendly and Meyer, 2015). Cohen's Kappa (κ) is a commonly used measure of agreement that compares the observed agreement to agreement expected by chance if the two observer's ratings were independent. If p_{ij} is the probability that a randomly selected subject is rated in category i by the first observer and in category j by the other, then the observed agreement is the sum of the diagonal entries, $P_0 = \sum_i p_{ii}$. If the ratings were independent, this probability of agreement (by chance) would be the sum of the products of the corresponding row totals and column totals, $P_c = \sum_i p_{i+} p_{+i}$. Here, row totals p_{i+} and column totals p_{+j} are marginal frequencies for observations i and j, respectively, so, $p_{i+} = \sum_j p_{ij}$ and $p_{+j} = \sum_i p_{ij}$. Cohen's κ is then the ratio of the difference between actual agreement and chance agreement, $P_0 - P_c$, to the maximum value this difference could obtain:

$$\kappa = \frac{P_0 - P_c}{1 - P_c} \quad (3)$$

When agreement is perfect, κ = 1; when agreement is no better than would be obtained from statistically independent ratings, κ = 0. Coefficient κ could conceivably be negative, but this rarely occurs in practice. The minimum possible value depends on the marginal totals. The original (unweighted) κ only counts strict agreement (the same category is assigned by both observers). A weighted version of κ may be used when one wishes to allow for partial agreement. Weighted κ uses weights, $0 \le w_{ij} \le 1$ for each cell in the table, with $w_{ii} = 1$ for the diagonal cells. In this case P_0 and P_c are defined as weighted sums:

$$P_0 = \sum_i \sum_j w_{ij} p_{ij} \quad (4)$$

$$P_c = \sum_i \sum_j w_{ij} p_{i+} p_{+j}. \quad (5)$$

For a $r \times r$ contingency table, two commonly-used patterns of weights are used, namely those based on equal spacing of weights (linear weighting) for a near-match,

$$w_{ij} = 1 - \frac{|i - j|}{r - 1} \quad (6)$$

and Fleiss-Cohen weights (quadratic weighting), based on an inverse-square spacing,

$$w_{ij} = 1 - \frac{|i - j|^2}{r - 1}. \quad (7)$$

For estimation of Kappa coefficient, the VassarStats-Website for Statistical Computation (Lowry, 2017) was used.

The Landis and Koch (1977) classification of the Kappa coefficient was used to assess the strength of agreement. The following classes of the strength of agreement are distinguished in this classification: poor (Kappa coefficient < 0.00), slight (0.00 ≤ Kappa coefficient < 0.20), fair (0.20 ≤ Kappa coefficient < 0.40), moderate (0.40 ≤ Kappa coefficient < 0.60), substantial (0.6 ≤ Kappa coefficient < 0.80), and almost perfect (0.8 ≤ Kappa coefficient ≤ 1.00).

RESULTS AND DISCUSSION

Characteristics of the extent and persistence of actual SWR of clay loam soil under *Pinus pinaster* trees at Ciavolo, Italy (CiF), sandy soil under *Pinus sylvestris* trees at Culbin, UK (CuF), silty clay soil under *Pinus halepensis* trees at Javea, Spain (JaF), and sandy soil under *Pinus sylvestris* trees at Sekule, Slovakia (SeF), as well as the extent and persistence of potential SWR of sandy soil samples taken under *Pinus syl-*

vestris trees at Culbin, UK, and estimated in the laboratory after oven-drying at 60°C (CuD), are presented in Table 2.

According to the classification proposed by Dekker et al. (2000), it was found that two of three pine species observed in this study induced strong (*Pinus pinaster* trees in clay loam soil at CiF site) to severe (*Pinus sylvestris* trees in sandy soil at CuD and SeF sites) SWR. *Pinus halepensis* trees induced slight SWR in silty clay soil at JaF site. This result is in agreement with the findings of Rodriguez-Alleres and Benito (2011) who found slight to severe repellency in sandy loam soil under *Pinus pinaster* trees at Fontáns, NW Spain. Sandy soil at Culbin, UK, was wettable under field conditions (0.104 ± 0.014 g g^{-1}, gravimetric water content) and became severely repellent after drying in the laboratory. It is in agreement with the findings of Dekker and Ritsema (1994), de Jonge et al. (1999) and Dekker et al. (2001) that SWR increases with a decrease in water content and that the soil becomes wettable above a certain water content called the critical water content. Mean values of RI and RI_c increase in the order: JaF < CuF < CiF < CuD < SeF. Mean values of WDPT increased in nearly the same order: CuF < JaF < CiF < CuD < SeF (Table 2). Thus the pine trees affected the extent and persistence of soil water repellency to a similar extend independently of the different soil and climate characteristics.

Regression dependence between RI/RI_c and WDPT

Table 3 shows the fitting results of several models that were considered to estimate the regression dependence between RI/RI_c and WDPT. Among the models fitted, the linear model yields the highest R-Squared value with 83.56%. The output shows the results of fitting a linear model to describe the relationship between RI (resp. RI_c) and WDPT. The equations of the fitted models are:

$$RI = 3.33 + 0.0626\ WDPT \qquad (8)$$

$$RI_c = 4.73 + 0.0509\ WDPT \qquad (9)$$

that are characterized by *P* values lower than 0.01, indicating a statistically significant relationship between RI and WDPT (as well as between RI_c and WDPT) at the 99% confidence level. The R-Squared statistic indicates that the model as fitted explains 83.56% of the variability in RI (resp. 83.64% in RI_c). The correlation coefficient equals 0.914 (0.915), thus indicating a relatively strong relationship between the variables. The relationship between WDPT and RI presented as Eq. (8) is in agreement with that presented by Blanco-Canqui and Lal (2009). Their relationship, found across 11 soils in eastern USA (RI = 0.761 + 0.337 WDPT (R^2 = 0.15)), is also linear, but the parameters are different.

The standard deviation of the residuals is 11.87 (9.61). This value can be used to construct prediction limits for new observations (Fig. 1). Similar statistical results were obtained for RI and RI_c, but equation (8) gives a higher range, and therefore RI_c will be used in our next evaluations.

The empirical data series RI_c were not normally distributed. The theoretical lognormal probability distributions of soil water repellency index estimated by STATGRAPHICS Plus software are depicted in Fig. 2. Several tests were conducted to determine whether statistically significant differences between the empirical and theoretical distributions occurred.

Table 2. Characteristics of the extent (RI and RI_c) and persistence (WDPT) of actual SWR at Ciavolo, Italy (CiF), Culbin, UK (CuF), Javea, Spain (JaF), and Sekule, Slovakia (SeF), as well as of potential SWR at Culbin, UK (CuD).

Site	Attribute	Minimum	Maximum	Median	Mean	Standard deviation	Skewness	Kurtosis	Number of replicates
CiF	WDPT (s)	47	1088	397	443	335	0.68	0.24	9
	RI (–)	11.4	45.2	17.8	22.7	12.3	1.06	–0.25	9
	RI_c (–)	5.9	70.6	18.6	23.6	15.3	1.57	2.77	81
CuF	WDPT (s)	1	1	1	1	0	–	–	9
	RI (–)	0.36	10.06	2.54	3.45	3.03	1.42	2.14	9
	RI_c (–)	0.29	18.47	2.50	3.34	3.40	2.68	8.08	81
CuD	WDPT (s)	94.2	2293	682.2	800.4	501.2	1.38	2.44	27
	RI (–)	7.03	67.6	26.1	26.2	18.4	1.51	2.89	9
	RI_c (–)	6.62	67.6	24.9	25.5	14.8	0.84	0.31	81
JaF	WDPT (s)	1	18	3	8	16	1.41	1.32	29
	RI (–)	0.71	2.95	1.78	1.73	0.73	0.10	–0.90	10
	RI_c (–)	0.43	6.21	1.49	1.92	1.29	1.41	1.70	100
SeF	WDPT (s)	8	7100	425.5	1256	1928	2.18	4.21	22
	RI (–)	3.57	360.2	38.6	100.4	122.4	1.29	0.72	11
	RI_c (–)	2.75	518.7	39.5	79.3	104.4	2.30	5.61	121

Table 3. Comparison of alternative models to fit the RI versus WDPT data.

Model	Correlation (–)	R-Squared (%)
Linear	0.9141	83.56
Square root-Y	0.9049	81.89
Multiplicative	0.8809	77.60
Square root-X	0.8592	73.83
Exponential	0.7701	59.30
Logarithmic-X	0.7500	56.25
Double reciprocal	0.5671	32.16
Reciprocal-X	–0.3400	11.56

It was found that the histograms of RI_c for CuF and JaF data fitted well with a lognormal distribution, while the histograms prepared from CiF, CuD and SeF data have rather a multimodal character (Fig. 2). The multimodal character of histograms prepared from CiF, CuD and SeF data is likely explained by the heterogeneous mixture of organic compounds with hydrophilic and hydrophobic functional groups forming the soil organic matter (Ellerbrock et al., 2005). The compounds were likely derived from hydrophobic tissue and exudates produced by microbes, algae and cyanobacteria, epicuticular waxes detached from pine needles and aliphatic compounds releasing from pine roots (Doerr et al., 2000).

Box-and-Whisker plot of the RI_c data series (Fig. 3) shows important features about the measured data. It is clear that the data range is very large. Series RI_c (and RI) does not have a normal distribution. Therefore, we cannot use Eqs (8) and (9) corresponding to the WDPT thresholds to determine the thresholds of RI_c (or RI).

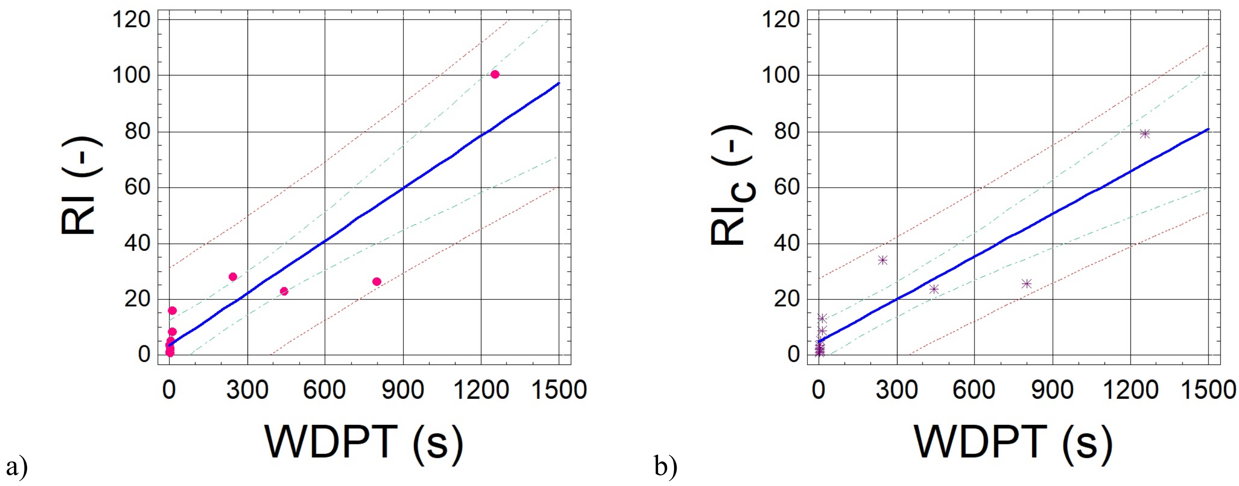

Fig. 1. Plot of fitted model (simple regression) a) RI vs. WDPT, b) RI_c vs. WDPT. The plot includes both 95% confidence limits (green lines) for the means (middle blue line) and 95% prediction limits (outer dotted red lines).

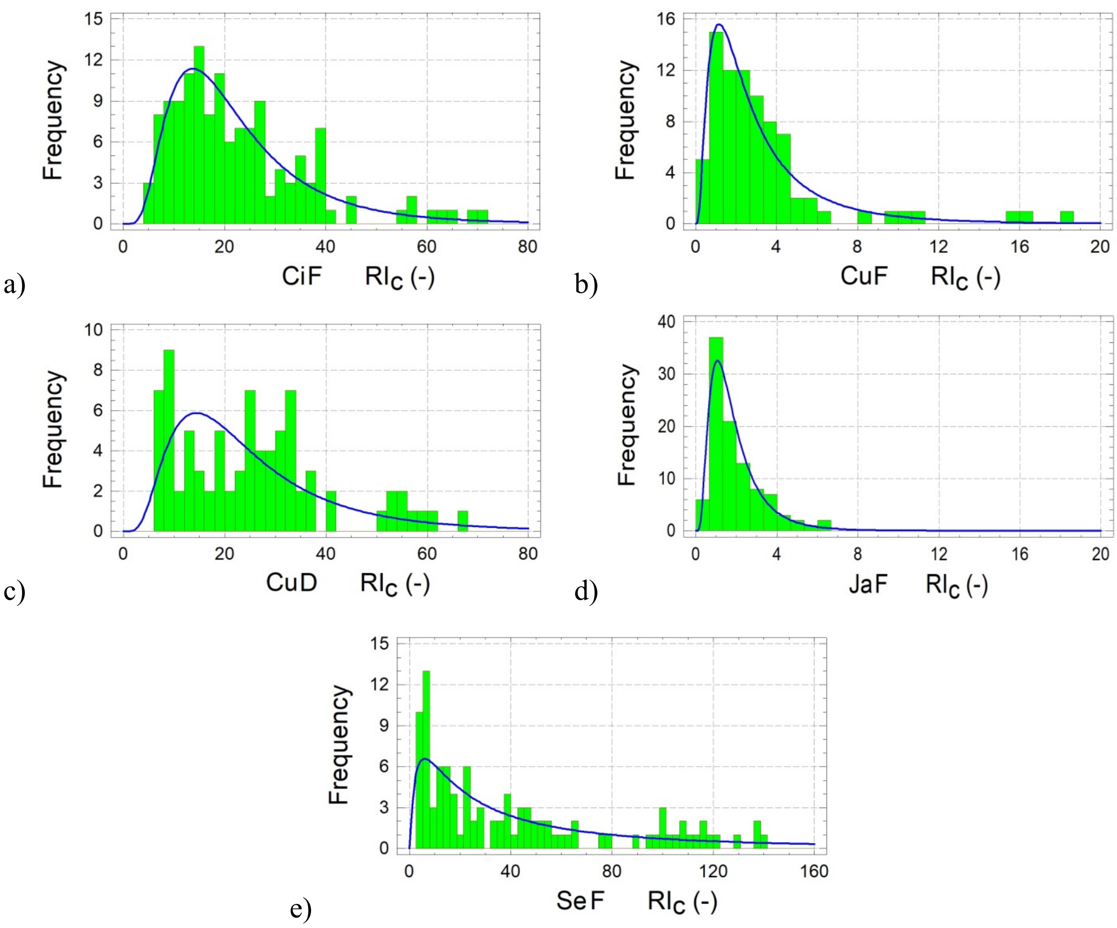

Fig. 2. Histograms and lognormal probability distribution curves of repellency index RI_c estimated at: a) Ciavolo, Italy (CiF); b) Culbin, UK, actual SWR (CuF); c) Culbin, UK, potential SWR (CuD); d) Javea, Spain (JaF); e) Sekule, Slovakia (SeF).

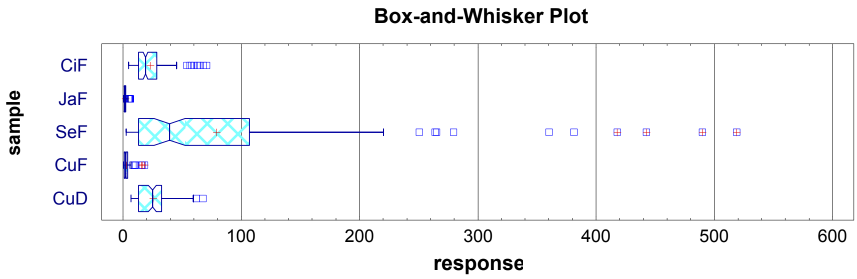

Fig. 3. Box-and-Whisker plots of repellency index RI_c estimated in situ at Ciavolo, Italy (CiF), Javea, Spain (JaF), Sekule, Slovakia (SeF), and Culbin, UK under both actual (CuF) and potential (CuD) SWR conditions (Mean marker – red cross, outlier symbols – blue squares, median – line in the rectangle).

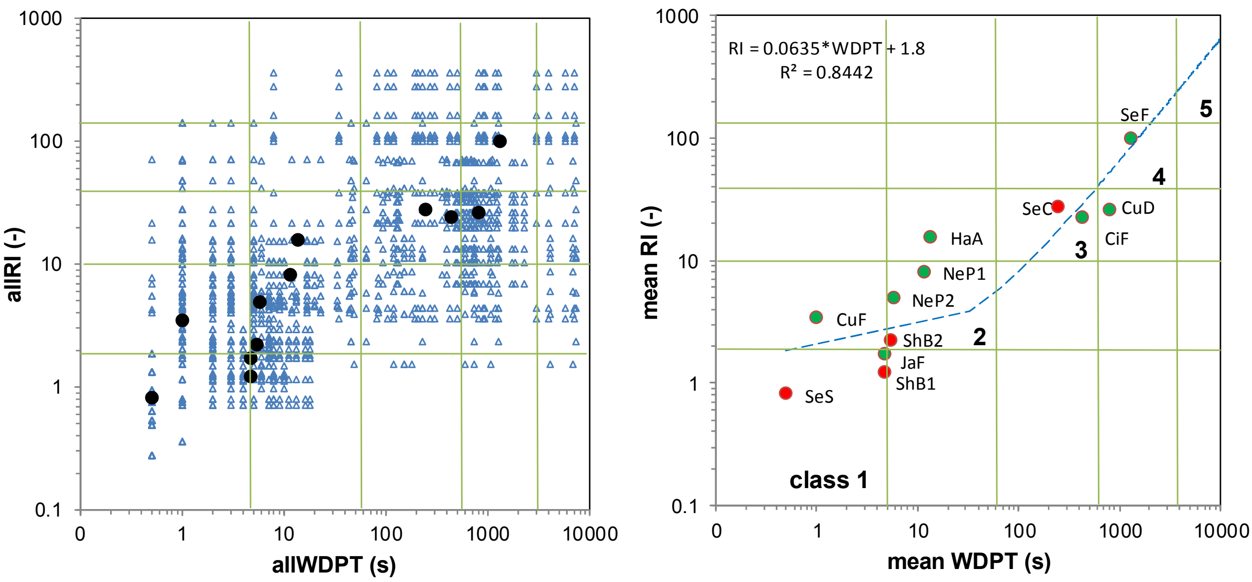

Fig. 4. a) Combined values of allWDPT and allRI data (blue triangles), mean WDPT and mean RI (black points) from each individual experimental site. b) Threshold lines between classes, and linear relationship between mean of RI and mean of WDPT from 12 localities. (Green points: cultivated soils, Red points: bare soils).

Determining thresholds for RI classes

Twelve sets of WDPT and RI values, measured both *in situ* at each of 11 experimental sites and in the laboratory for the dried pine-forest soil taken at Culbin, UK, were combined with one another and 2473 pairs of values (allWDPT, allRI) were obtained (Fig. 4a). The thresholds for five RI classes, corresponding to five WDPT classes were estimated as follows:

1. First, the parameters of theoretical lognormal distribution of the allWDPT data were estimated.
2. Then, the probabilities for tail areas were calculated for the fitted lognormal distribution of allWDPT series. The tail area for allWDPT threshold below 5 s had the probability P = 0.40; tail area below 60 s, P = 0.72; tail area below 600 s, P = 0.93; and tail area below 3600 s had the probability P = 0.98.
3. Next, the threshold values for five classes of the allRI series were estimated from the theoretical lognormal distribution of allRI series, using the probabilities calculated above.
4. Finally, the computed values were adjusted and the final thresholds are presented in Table 4.

The adapted linear relationship between 12 pairs of mean RI and mean WDPT values together with the threshold lines between classes is presented in Fig. 4b.

In the next step, the pairs of allWDPT and allRI were ranked in five classes based on the threshold values in Table 4 and two categorical variables were created, $WDPT_{class}$ and RI_{class} with categorical values 1, 2, 3, 4, and 5. A contingency table of the categorical pairs of $WDPT_{class}$ and RI_{class} is presented in Table 5. The table gives us the frequencies of observations cross-classified by the two variables.

Table 4. Thresholds of the repellency index RI classes corresponding water drop penetration time WDPT classes, and their descriptive labels.

class	descriptive labels	WDPT thresholds (s)	RI thresholds (–)
1	wettable or non-water-repellent soil	WDPT < 5	RI < 1.95
2	slightly water repellent soil	5 ≤ WDPT < 60	1.95 ≤ RI < 10
3	strongly water repellent soil	60 ≤ WDPT < 600	10 ≤ RI < 50
4	severely water repellent soil	600 ≤ WDPT < 3600	50 ≤ RI < 110
5	extremely water repellent soil	3600 ≤ WDPT	110 ≤ RI

To test whether some associations exist, to quantify the strength of association, and to understand the nature of the association among these variables, a three-dimensional histogram of the $WDPT_{class}$ and RI_{class} variables was created (Fig. 5a) from the data of contingency table (Table 5). The compliance between RI_{class} and $WDPT_{class}$ pairs is visually presented in the weighted agreement chart in Fig. 5b (Friendly and Meyer, 2015; Papierowska et al., 2018). The red squares represent the likelihood of ranking in the same class for both variables and corresponds to exact agreement in classification (for example, for class 3 the likelihood is 33). The yellow rectangles correspond to the likelihood of ranking in the same or neighbour class, i.e., partial agreement (e.g., for class 3 it is: 33, 32, 34, 23, and 43). White rectangles represent the likelihood of other rankings.

Behaviour of the characteristics was used to verify the dependence between $WDPT_{class}$ and RI_{class} classes (Table 5). First, the Chi-Square test was used to determine whether both classifications (i.e., row and column in the contingency table) are independent. Since $P < 0.01$, the hypothesis that rows and columns are independent can be rejected at the 99% confidence level. Therefore, the observed row (RI_{class}) for a particular case is related to its column ($WDPT_{class}$).

Then, we estimated the contingency coefficient and lambda of the contingency Table 5. These characteristics express the degree of association on a scale of 0 to 1. Lambda measures how useful the row or column factor is in predicting the other factor. The value of lambda with columns dependent equals 0.0525. This means that there is a 5.25% reduction in error when rows (RI) are used to predict columns (WDPT). For those statistics with P values, P values less than 0.05 indicate a significant association between rows RI and columns WDPT at the 95% confidence level. Contingency coefficient (a version of a Chi-Square test that measures the strength of the dependency between two characteristics) obtained value of 0.5899.

Finally, we computed Kappa coefficient, which provides a measure of the degree to which two judges, $WDPT_{class}$ and RI_{class} concur in their respective sorting's of 5 items into r mutually exclusive categories. Three different versions of Kappa coefficient were calculated, the values according to Eqs. 3–7, and following values of Kappa coefficient were obtained:

- Cohen's unweighted Kappa coefficient = 0.304,
- Kappa coefficient with linear weighting = 0.429,
- Kappa coefficient with quadratic weighting = 0.533.

According to the Landis and Koch (1977) classification of Kappa coefficient, the strength of agreement for the mean WDPT and mean RI pairs is fair for the Cohen's unweighted Kappa coefficient, and moderate for both the Kappa coefficient with linear weighting and the Kappa coefficient with quadratic weighting.

Moreover, we also estimated Kappa coefficient for the mean WDPT and mean RI pairs (contingency table according to Fig. 4b):

- Cohen's unweighted Kappa coefficient = 0.660,
- Kappa coefficient with linear weighting = 0.775,
- Kappa coefficient with quadratic weighting = 0.875.

According to the Landis and Koch (1977) classification of Kappa coefficient, the strength of agreement for the mean WDPT and mean RI pairs is substantial for the Cohen's unweighted Kappa coefficient, substantial for the Kappa coefficient with linear weighting, and almost perfect for the Kappa coefficient with quadratic weighting.

Table 5. Contingency table of all repellency index RI_{class}, corresponding to water drop penetration time $WDPT_{class}$, their descriptive labels, and classes used in this study. (Red colour: exact agreement, yellow: partial agreement).

RI_{class}		$WDPT_{class}$				
		Class 1	Class 2	Class 3	Class 4	Class 5
Class	Value	< 5 s	5–60 s	60–600 s	600–3600 s	> 3600 s
1	<1.95	595	90	0	3	2
2	1.95–10	338	243	62	48	15
3	10–50	243	61	192	190	22
4	50–110	46	7	45	96	5
5	>110	32	14	42	36	46

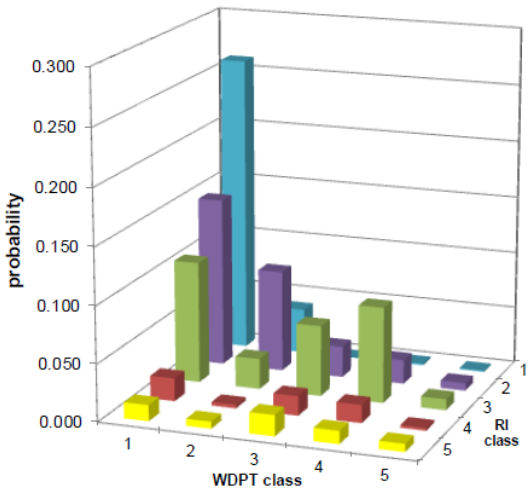

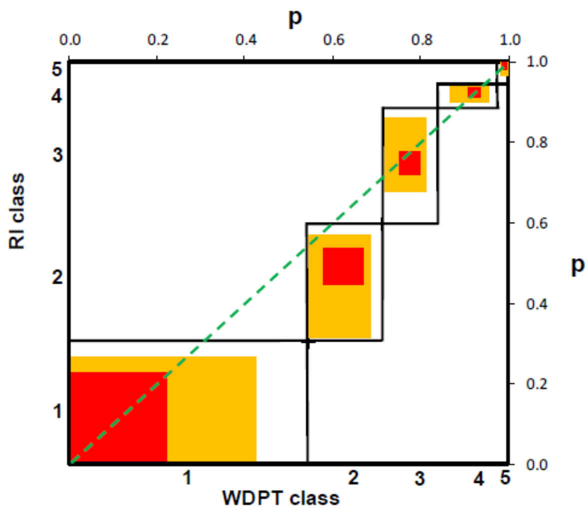

Fig. 5. a) Three-dimensional histogram of the contingency Table 5. b) Weighted agreement chart obtained by comparing $WDPT_{class}$ and RI_{class}. The red colour represents exact agreement and the yellow colour represents partial agreement.

CONCLUSIONS

Pine species observed in this study induced slight (*Pinus halepensis* trees in silty clay soil at Javea, Spain (JaF) site), strong (*Pinus pinaster* trees in clay loam soil at Ciavolo, Italy (CiF) site), and severe (*Pinus sylvestris* trees in sandy soil at Sekule, Slovakia (SeF) site) soil water repellency *in situ*. However, the sandy soil was wettable in situ at Culbin, United Kingdom (CuF), but became severely water repellent after oven-drying at 60°C. Mean values of WDPT increased in nearly the same order as mean values of RI and RI_c thus confirming that these indices are reliable in assessing the persistence (WDPT) and extent (RI and RI_c) of soil water repellency. While the histograms of repellency index RI_c prepared from CuF and JaF data can be fitted well with lognormal distribution, the histograms prepared from CiF, CuD and SeF data have rather a multimodal character due probably to the variable nature of hydrophobic coatings on soil particles and their spatial distribution in soils.

A large set of paired WDPT and RI values, measured both *in situ* and in the laboratory in twelve sites differing for soil type and land use, allowed to propose a new classification for the repellency index RI based on the WDPT classification. The comparability of RI and WDPT results was determined. It was found that the strength of agreement for the mean WDPT and mean RI pairs is substantial for the Cohen's unweighted Kappa coefficient, substantial for the Kappa coefficient with linear weighting, and almost perfect for the Kappa coefficient with quadratic weighting.

Acknowledgements. This work was supported by the Slovak Scientific Grant Agency VEGA Project Nos. 2/0054/14 and 2/0009/2015, the Slovak Research and Development Agency Project No. APVV-15-0160, and it results from the project implementation of the “Centre of excellence for integrated flood protection of land” (ITMS 26240120004).

REFERENCES

Alagna, V., Iovino, M., Bagarello, V., Mataix-Solera, J., Lichner, Ľ., 2017. Application of minidisk infiltrometer to estimate water repellency in Mediterranean pine forest soils. J. Hydrol. Hydromech., 65, 254–363.

Beatty, S.M., Smith, J.E., 2010. Fractional wettability and contact angle dynamics in burned water repellent soils. J. Hydrol., 391, 97–108.

Beatty, S.M., Smith, J.E., 2013. Dynamic soil water repellency and infiltration in post-wildfire soils. Geoderma, 192, 160–172.

Bens, O., Buczko, U., Sieber, S., Hüttl, R.F., 2006. Spatial variability of O layer thickness and humus forms under different pine beech-forest transformation stages in NE Germany. J. Plant Nutr. Soil Sci., 169, 5–15.

Bens, O., Wahl, N.A., Fischer, H., Hüttl, R.F., 2007. Water infiltration and hydraulic conductivity in sandy cambisols: impacts of forest transformation on soil hydrological properties. Eur. J. Forest Res., 126, 101–109.

Blanco-Canqui, H., Lal, R., 2009. Extent of soil water repellency under long-term no-till soils. Geoderma, 149, 171–180.

Buczko, U., Bens, O., Fischer, H., Hüttl, R.F., 2002. Water repellency in sandy luvisols under different forest transformation stages in northeast Germany. Geoderma, 109, 1–18.

Buczko, U., Bens, O., Hüttl, R.F., 2005. Variability of soil water repellency in sandy forest soils with different stand structure under Scots pine (*Pinus sylvestris*) and beech (*Fagus sylvatica*). Geoderma, 126, 317–336.

Buczko, U., Bens, O., Hüttl, R.F., 2006. Water infiltration and hydrophobicity in forest soils of a pine–beech transformation chronosequence. J. Hydrol., 331, 383–395.

CAB International, 2002. Pines of Silvicultural Importance. CABI Publishing, Wallingford.

Decagon, 2012. Mini Disk Infiltrometer User’s Manual, Version 10. Decagon Devices, Inc., Pullman, 18 p.

Diehl, D., 2013. Soil water repellency: Dynamics of heterogeneous surfaces. Colloids and Surfaces A: Physicochem. Eng. Aspects, 432, 8–18.

de Jonge, L.W., Jacobsen, O.H., Moldrup, P., 1999. Soil water repellency: effects of water content, temperature, and particle size. Soil Sci. Soc. Am. J., 63, 437–442.

Dekker, L.W., Ritsema, C.J., 1994. How water moves in a water repellent sandy soil. 1. Potential and actual water repellency. Water Resources Research, 30, 2507–2517.

Dekker, L.W., Ritsema, C.J., Oostindie, K., 2000. Extent and significance of water repellency in dunes along the Dutch coast. J. Hydrol., 231–232, 112–125.

Dekker, L.W., Doerr, S.H., Oostindie, K., Ziogas, A.K., Ritsema, C.J., 2001. Water repellency and critical soil water content in a dune sand. Soil Sci. Soc. Am. J., 65, 1667–1674.

Doerr, S.H., 1998. On standardizing the “Water Drop Penetration Time" and the "Molarity of an Ethanol Droplet" techniques to classify soil hydrophobicity: a case study using medium textured soils. Earth Surf. Process. Landforms, 23, 663–668.

Doerr, S.H., Shakesby, R.A., Walsh, R.P.D., 2000. Soil water repellency: its causes, characteristics and hydro-geomorphological significance. Earth-Sci. Rev., 51, 33–65.

Ellerbrock, R.H., Gerke, H.H., Bachmann, J., Goebel, M.-O., 2005. Composition of organic matter fractions for explaining wettability of three forest soils. Soil Sci. Soc. Am. J., 69, 57–66.

Fér, M., Leue, M., Kodešová, R., Gerke, H.H., Ellerbrock, R.H., 2016. Droplet infiltration dynamics and soil wettability related to soil organic matter of soil aggregate coatings. J. Hydrol. Hydromech., 64, 111–120.

Flores-Mangual, M.L., Lowery, B., Bockheim, J.G., Pagliari, P.H., Scharenbroch, B., 2013. Hydrophobicity of Sparta sand under different vegetation types in the Lower Wisconsin River Valley. Soil Sci. Soc. Am. J., 77, 1506–1516.

Friendly, M., Meyer, D., 2015. Discrete Data Analysis with R: Visualization and Modeling Techniques for Categorical and Count Data. Chapman & Hall. ISBN 9781498725835. Web site for book: ddar.datavis.ca

Garcia, F.J.M., Dekker, L.W., Oostindie, K., Ritsema, C.J., 2005. Water repellency under natural conditions in sandy soils of southern Spain. Aust. J. Soil Res., 43, 291–296.

Gee, G.W., Bauder, J.W., 1986. Particle-size analysis. In: Klute, A. (Ed.): Methods of Soil Analysis, Part 1: Physical and Mineralogical Methods. Agron. Monogr. 9. 2nd ed. ASA and SSSA, Madison, WI, pp. 383–411.

Gerke, H.H., Hangen, E., Schaaf, W., Hűttl, R.F., 2001. Spatial variability of potential water repellency in a lignitic mine soil afforested with *Pinus nigra*. Geoderma, 102, 255–274.

Haas, C., Gerke, H.H., Ellerbrock, R.H., Hallett, P.D., Horn, R., 2018. Relating soil organic matter composition to soil water repellency for soil biopore surfaces different in history from two Bt horizons of a Haplic Luvisol. Ecohydrology, 11, Article Number: e1949. https://doi.org/10.1002/eco.1949

Hallett, P.D., Baumgartl, T., Young, I.M., 2001. Subcritical water repellency of aggregates from a range of soil management practices. Soil Sci. Soc. Am. J., 65, 184–190.

Hallett, P.D., Nunan, N., Douglas, J.T., Young, I.M., 2004. Millimeter-scale spatial variability in soil water sorptivity: scale, surface elevation, and subcritical repellency effects. Soil Sci. Soc. Am. J., 68, 352–358.

Islam, K.K., Patricia, S., Rinchen, Y., 2011. Broadleaved regeneration dynamics in the Pine plantation. Journal of Forest

Science, 57, 432–438.
Janusauskaite, D., Baliuckas, V., Dabkevicius, Z., 2013. Needle litter decomposition of native *Pinus sylvestris* L. and alien *Pinus mugo* at different ages affecting enzyme activities and soil properties on dune sands. Baltic Forestry, 19, 50–60.
Keck, H., Felde, V.J.M.N.L., Drahorad, S.L., Felix-Henningsen, P., 2016. Biological soil crusts cause subcritical water repellency in a sand dune ecosystem located along a rainfall gradient in the NW Negev desert, Israel. J. Hydrol. Hydromech., 64, 133–140.
Kottek, M., Grieser, J., Beck, C., Rudolf, B., Rubel, F., 2006. World map of the Köppen-Geiger climate classification updated. Meteorologische Zeitschrift, 15, 259–263.
Krueger, J., Heitkötter, J., Leue, M., Schlüter, S., Vogel, H.-J., Marschner, B., Bachmann, J., 2018. Coupling of interfacial soil properties and bio-hydrological processes: The Flow Cell Concept. Ecohydrology, 11, Article Number: e2024. https://doi.org/10.1002/eco.2024
Landis, J.R., Koch, G.G., 1977. The measurement of observer agreement for categorical data. Biometrics, 33, 159–174. URL: http://www.jstor.org/stable/2529310
Lichner, Ľ., Hallett, P.D., Feeney, D., Ďugová, O., Šír, M., Tesař, M., 2007. Field measurement of the impact of hydrophobicity on soil water transport under different vegetation over time. Biologia, 62, 537–541.
Lichner, L., Hallett, P.D., Orfánus, T., Czachor, H., Rajkai, K., Šír, M., Tesař, M., 2010. Vegetation impact on the hydrology of an aeolian sandy soil in a continental climate. Ecohydrology, 3, 413–420.
Lichner, Ľ., Holko, L., Zhukova, N., Schacht, K., Rajkai, K., Fodor, N., Sándor, R., 2012. Plants and biological soil crust influence the hydrophysical parameters and water flow in an aeolian sandy soil. J. Hydrol. Hydromech., 60, 309–318.
Lichner, Ľ., Capuliak, J., Zhukova, N., Holko, L., Czachor, H., Kollár J., 2013. Pines influence hydrophysical parameters and water flow in a sandy soil. Biologia, 68, 1104–1108.
Lichner, Ľ., Rodný, M., Schacht, K., Marschner, B., Chen, Y., Nadav, Y., Tarchitzky, J., 2017. Comparison of various techniques to estimate the extent and persistence of soil water repellency. Biologia, 72, 982–987.
Lichner, L., Felde, V.J.M.N.L., Büdel, B., Leue, M., Gerke, H.H., Ellerbrock, R.H., Kollár, J., Rodný, M., Šurda, P., Fodor, N., Sándor, R., 2018. Effect of vegetation and its succession on water repellency in sandy soils. Ecohydrology, 11, Article Number: e1991. https://doi.org/10.1002/eco.1991
Lowry, R., 2017. VassarStats - Website for Statistical Computation. http://vassarstats.net/index.html
Orfánus, T., Hallett, P.D., Bedrna, Z., Lichner, Ľ., Kňava, K., Sebíň, M., 2008. Small-scale variation of hydraulic properties in pine forest soil near Sekule, southwestern Slovakia. Soil Water Res., 3, S123–S129.
Ovington, J.D., 1950. The afforestation of Culbin Sands. Journal of Ecology, 38, 303–319.
Papierowska, E., Matysiak, W., Szatyłowicz, J., Debaene, G., Urbanek, E., Kalisz, B., Łachacz, A., 2018. Compatibility of methods used for soil water repellency determination for organic and organo-mineral soils. Geoderma, 314, 221–231.
Pekárová, P., Pekár, J., Lichner, Ľ., 2015. A new method for estimating soil water repellency index. Biologia, 70, 1450–1455.
Philip, J.R., 1957. The theory of infiltration: 1. The infiltration equation and its solution. Soil Science, 83, 345–358.
Rodriguez-Alleres, M., Benito, E., 2011. Spatial and temporal variability of surface water repellency in sandy loam soils of NW Spain under *Pinus pinaster* and *Eucalyptus globulus* plantations. Hydrol. Process., 25, 3649–3658.
Rumpel, C., Knicker, H., Kögel-Knabner, I., Skjemstad, J.O., Hüttl, R.F., 1998. Types and chemical composition of organic matter in reforested lignite-rich mine soils. Geoderma, 86, 123–142.
Siteur, K., Mao, J., Nierop, K.G.J., Rietkerk, M., Dekker, S.C., Eppinga, M.B., 2016. Soil water repellency: a potential driver of vegetation dynamics in coastal dunes. Ecosystems, 19, 1210–1224.
Soil Survey Staff, 2014. Keys to Soil Taxonomy. 12th ed. NRCS, Washington, DC.
Statgraphics, 2014. STATGRAPHICS Centurion XVII User Manual, 311pp. Statpoint Technologies, Inc., The Plains, Virginia, USA. www.STATGRAPHICS.com
Ward, P.R., Roper, M.M., Jongepier, R., Micin, S.F., 2015. Impact of crop residue retention and tillage on water infiltration into a water-repellent soil. Biologia, 70, 1480–1484.
Will, G.M., Raliard, P., 1976. Radiata pine - soil degrader or improver? N.Z. Journal of Forestry, 21, 248–252.

Received 22 January 2018
Accepted 17 May 2018